

# BUBBLE BEHAVIOR IN BUBBLING FLUIDIZED BEDS OF BINARY PARTICLES

HIROYUKI KAGE, HISAMORI YAMAGUCHI, HIROYUKI ISHII  
AND YOSHIZO MATSUNO

*Department of Applied Chemistry, Kyushu Institute of Technology,  
Kitakyushu 804*

**Key Words:** Fluidization, Optic Fiber Probe, Bubble Size, Bubble Rising Velocity, Incipient Bubble Diameter, Maximum Bubble Diameter

Sizes and rising velocities of bubbles in a gas fluidized bed composed of two kinds of particles of different sizes but of the same density were observed by optic fiber probes. In all, three kinds of particles were used for the measurement of bubble behavior. The bubble growth ratio showed a minimum at 0.4 mass fraction of the finer of the two kinds of component particles. Bubble diameters showed a linear change with the height of rise above the distributor up to the maximum attainable diameter, and then remained constant. The bubble growth ratio can be correlated better by the bubble rising velocity, which is regarded as one kind of index of the fluidity of the bed particles, rather than by the mass fraction of the particle. Bubble growth is strongly correlated with the bubble rising velocity, and both seem to be controlled by the fluidity of the bed particles. On the basis of the results obtained, a method for determining the bubble diameter in the system of two kinds of component particles at any height was proposed.

## 1. Introduction

A longstanding but still current topic is the estimation of bubble diameters and velocities in order to construct a bubble model for designing and scaling up a gas-solid fluidized bed, so as to determine the values of fluidization characteristics necessary for understanding such phenomena as chemical reactions, heat and mass transfers and the like. Mori and Wen<sup>1,4)</sup> proposed an efficient correlation, including the effect of bed diameter on bubble behavior, by which the bubble diameters against the height above the distributor can be estimated within  $\pm 50\%$  error in reference to previous experimental data.

Usually the particles in beds used in industry are subject to size variation due to attrition among particles and/or between particles and the wall, and show their own distributions.

In this work, by using a bed composed of particles of two kinds (glass beads of different diameters) and systematically changing the weight fraction of particles and the gas velocity, a simple method of correlating bubble diameter is proposed for the two-component fluidized bed system.

## 2. Experimental Equipment and Procedure

Figure 1 is a diagram of the experimental equipment. The fluidized bed, made of polyvinyl chloride, was

146 mm in inner diameter and 850 mm in height. The distributor was a perforated plate with 19 holes (2 mm  $\phi$ ) and 30 mm triangular pitch, which corresponds to 0.356% opening ratio. An optic fiber method<sup>7)</sup> was adopted to measure bubble diameters and velocities. Two pairs of optic probes, one of which was composed of an acceptor and a light source, were set 40 mm apart along the center of the bed axis. The distance between the tips of acceptor and light source was 10 mm. The detector, which received light signals from the acceptor, transformed the output voltages from 0 to 10 V on a recorder. The signals from the probes were recorded on a floppy disk, and were subsequently transferred to a main computer through an A/D converter. These converted signals were digitized and, using the cross-correlation

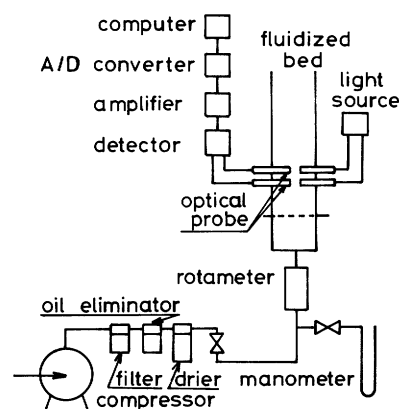


Fig. 1. Experimental equipment

\* Received December 25, 1990. Correspondence concerning this article should be addressed to H. Kage. H. Yamaguchi is now with Imprex Systems Inc., Kitakyushu 804. H. Ishii is now with Idemitsu Engineering Co., Ltd., Chiba 260.

function programmed in the main computer, were analyzed to determine the time lag for a bubble to pass from the lower probe to the upper probe. The number of sampling points was 1024 for 5.12 s per channel. From this sampling set, about ten to twenty pulses were gained to determine the rising velocity of bubble  $u_b$ . The  $u_b$  is the quotient of the distance between the upper and lower tips divided by the time lag of corresponding pulses of the bubbles.

Three kinds of glass beads (coarse, middle, and fine) of 2520 kg/m<sup>3</sup> in density were used as bed particles. Their diameters were 28–32# (average diameter = 542  $\mu$ m), 80–100# (163  $\mu$ m) and 250–270# (58  $\mu$ m) respectively. Experiments were made by mixing two of these three kinds of particles to adjust the weight percentages of finer particles  $F_0$  to 20, 40, 60, and 80 wt%, and also by preparing single particles ( $F_0=0$  and 100) in order to compare the results of each combination of two kinds of component particles. The total weight of particles was kept to 20 kg in the main experiments. The measured minimum fluidization velocities of these systems are tabulated in **Table 1**.

For every set of two (or one) kinds of component particles the measurement was repeated by changing the superficial gas velocity  $u_0$  at seven heights above the distributor by use of the optic fiber probe method.

### 3. Preliminary Experiment for Determination of Bubble Diameter

#### 3.1 Reliability of optic fiber probe

First, a two-dimensional fluidized bed was used to determine whether or not the optic probes exactly measure the bubble diameter. Rowe and Masson<sup>17)</sup> had pointed out that the insertion of probes in the bed, especially with a horizontal supporting stem, deformed the bubble shape and changed the rising velocity. Therefore, we investigated whether or not the existence of probes remarkably influenced the bubble behavior. The two-dimensional bed used was made of transparent acrylic resin and was 25 cm wide, 1 cm thick and 100 cm high. The distributor had seven holes (2 mm $\phi$ ) bored in a line, with 40 mm pitch and 0.88% opening ratio. The total weight of particles charged was 4 kg.

The bubble heights were observed from the signals through optic fiber probes set at 74 and 78 cm above the distributor. Then pictures were taken by a motor-driven 35 mm camera at about 70 to 80 cm under the same experimental conditions, and the results from the two methods were compared.

By visual observation, there was almost no recognizable difference in bubble size owing to the presence of probes. In fact, bubble heights measured by both the optic probes and by photographs agreed well, as will be mentioned later. Therefore, we judged the effect of the insertions of probes and the horizontal

**Table 1.** Adopted systems and minimum fluidization velocities

(a) Single-component particles

System	$d_p$ [ $\mu$ m]	$u_{mf}$ [m/s]
Coarse	542	0.209
Middle	163	0.0280
Fine	58	0.0076

(b) Two-component particles

	$F_0$ [wt%]	$u_{mf}$ [m/s]	$u'_{mf}$ [m/s]	$E$ [%]
A	20	0.064	0.0634	-0.51
	40	0.013	0.0251	48.1
	60	0.0056	0.0129	56.6
	80	0.0072	0.0086	17.1
B	20	0.062	0.101	38.8
	40	0.034	0.0577	41.1
	60	0.031	0.0386	19.7
	80	0.024	0.0303	20.8
C	20	0.015	0.0173	13.3
	40	0.0080	0.0120	33.3
	60	0.0081	0.0092	12.3
	80	0.0061	0.0079	22.8

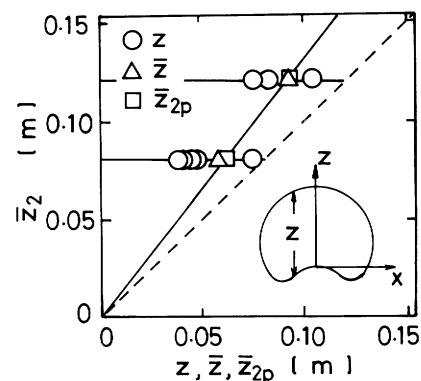


**Fig. 2.** Relationship between  $\bar{z}_2$  and  $z$  in two-dimensional bed

supporting stems to be negligible.

The maximum height  $z_2$  of each bubble was measured on the photos and the  $\bar{z}_2$  was obtained by averaging  $z_2$ 's of at least ten bubbles. On the other hand, the products of  $u_b$  and the time shift between the signals from two probes gave us the intercepted chords of bubble,  $z$ , and these are plotted against  $\bar{z}_2$  in **Fig. 2**. In this figure, the mean values of several tens of intercepted chords,  $\bar{z}$ , are also plotted together. In **Fig. 2**, it is found that  $\bar{z}_2$  is larger than  $z$ . This means that the tip of the optic fiber does not necessarily record the maximum chord of the bubble. It is also observed that the values of  $z$  cover a wide scope and their maximum is almost equal to  $\bar{z}_2$ .

Next we tried to calculate the average height of each bubble recorded by photo, according to the following

equation.

$$z_{2p} = \sum tz\Delta x / \sum t\Delta x \quad (1)$$

where  $z$  is the height of the bubble at the abscissa  $x$ , and  $t$  is the thickness of the bed (here  $t$  is 1 cm). As shown in Fig. 2,  $\bar{z}_{2p}$  and  $\bar{z}$  agree well with each other, and this result shows that the optic probes exactly measure the intercepted chords of real bubbles. This further proves the probe insertion to be independent of the bubble deformation mentioned above.

The solid line in Fig. 2 represents the correlation between  $\bar{z}_2$  and  $\bar{z}_{2p}$  and is described by Eq. (2).

$$\bar{z}_2 = 1.32\bar{z}_{2p} = 1.32\bar{z} \quad (2)$$

### 3.2 Data treatment for determination of bubble diameter

As we had no measuring equipment, such as an X-ray device<sup>15,18</sup>, to directly watch the inside of the three-dimensional bed at hand, the analyses were based on the results of the near equality of  $\bar{z}$  with  $\bar{z}_{2p}$  mentioned in 3.1. With the use of a transparent three-dimensional fluidized bed, pictures of the bubble rising along the wall were taken. By deforming the bubble shape on the picture into a simple one as shown in Fig. 3(b) and assuming that the bubble volume is an ellipsoid (Fig. 3(c)) circling the axis  $z$ , then  $z_{3p}$  will be described as follows in the same manner as introduced in Eq. (1).

$$z_{3p} = \frac{V_b}{\int_0^{r_1} \int_0^\pi 2r d\theta dr} = \frac{\int_0^{r_1} \int_0^\pi 2rz d\theta dr}{\int_0^{r_1} \int_0^\pi 2r d\theta dr} \quad (3)$$

Here  $z$  is a surface curve of an axial-symmetric ellipsoid above  $z=0$  and is expressed by

$$z = a - br^c \quad (4)$$

where  $a$ ,  $b$  and  $c$  are constants which fit each deformed bubble shape, as determined by the method of least squares. Table 2 shows the comparison between  $z_{3p}$  and the maximum height in each bubble observed by the camera,  $z_3$ . The ratio of  $\bar{z}_3$  to  $\bar{z}_{3p}$  ranges between 1.25 and 1.35, the mean value being 1.30. Accordingly, Eq. (5) is obtained for the correlation among  $\bar{z}_3$ ,  $\bar{z}_{3p}$  and  $\bar{z}$  of a three-dimensional bed system.

$$\bar{z}_3 = 1.30\bar{z}_{3p} = 1.30\bar{z} \quad (5)$$

We also observed that there was almost no recognizable difference in rising bubble size owing to the existence of probes situated in the same manner as for the two-dimensional bed.

Further, in this work the bubble diameter  $D_b$  was defined by

$$D_b = (6V_b/\pi)^{1/3} \quad (6)$$

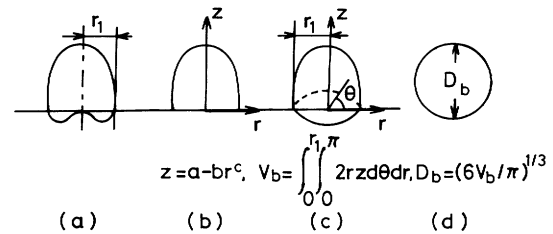


Fig. 3. Deformation of bubble shape to determine bubble diameter

Table 2. Bubble heights in three-dimensional bed

$\bar{z}_3$ by photo [m]	$\bar{z}_{3p}$ by Eq. (3) [m]	$\bar{z}_3/\bar{z}_{3p}$ [—]
0.030	0.022	1.35
0.040	0.032	1.25
0.050	0.040	1.26
0.070	0.053	1.31
0.090	0.070	1.29
0.140	0.107	1.31
0.170	0.130	1.31
Ave.		1.30

The data from the optic fiber probe were converted into  $D_b$  by Eqs. (3), (5) and (6).

## 4. Results and Discussion

### 4.1 Minimum fluidization velocity $u_{mf}$

Cheung *et al.*<sup>1)</sup> showed the minimum fluidization velocity of the two component particles  $u'_{mf}$  and gave

$$u'_{mf} = u_f(u_c/u_f)^{(100 - F_0/100)^2} \quad (7)$$

As shown in Table 1(b),  $u_{mf}$  agrees with  $u'_{mf}$  within about  $\pm 40\%$  with a few exceptions, and is found to be smaller than the values expected, except the 20% for  $F_0$  in system A. In our experiments,  $u_{mf}$  decreases more suddenly with the addition of finer particles and so the effect of the existence of finer particles can be observed remarkably at lower  $F_0$  than the results calculated by Eq. (7). The reason for the difference was not found, but  $u_{mf}$  obtained in this work may be usable for analysis in the light of the permissible resultant error from the equation of Cheung *et al.*

### 4.2 Bubble rising velocity

Figure 4 shows that  $u_b$ , which increases with  $h$ , attains a maximum at about 40 cm height and then remains constant. A typical plot for  $u_b$  with the change of  $F_0$  is shown in Fig. 5, in which a term related to the excess gas flow ( $u_0 - u_{mf}$ ) is selected as the abscissa by taking into account the variation of  $u_{mf}$  due to the change in  $F_0$ . By the choice of ( $u_0 - u_{mf}$ ) as the abscissa, the experimental results of each  $F_0$  approach each other closely as shown in Fig. 5, but the plotted data of each  $F_0$  do not stand in the order of  $F_0$ . Figure 5 suggests that the effect of  $F_0$  on  $u_b$  is not so simple.

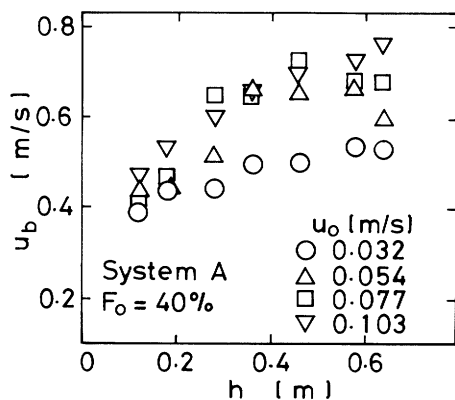


Fig. 4. Bubble rising velocity against  $h$

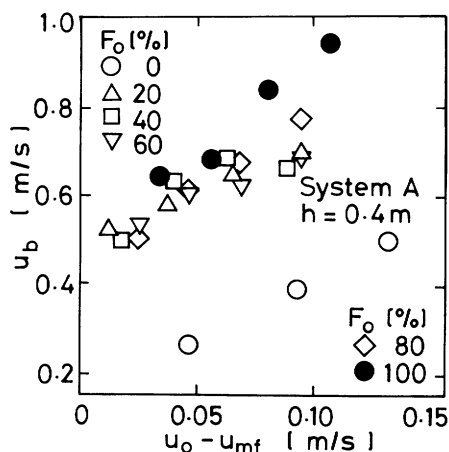


Fig. 5. Effect of  $F_0$  on  $u_b$

### 4.3 Bubble diameter

A typical change of  $D_b$  against  $h$  is shown in Fig. 6, taking  $u_0$  as a parameter.  $D_b$  increases linearly with  $h$  until it reaches a constant value of  $D_{bm}$  above which  $D_b$  cannot grow larger. The maximum attainable bubble diameter proposed by Leung<sup>11)</sup> exists clearly in our experimental results. However, this tendency is different from those found by Geldart<sup>4)</sup> and other investigators<sup>2,3,7,9,16)</sup>.

Miwa *et al.*<sup>13)</sup> derived the following equation for the incipient bubble diameter, assuming that the two-phase theory holds.

$$D_{b0} = 0.872 \{ A_t (u_0 - u_{mf}) / n_{or} \}^{0.4} \quad (8)$$

In Fig. 6, intercepts of solid lines at  $h=0$  show  $D_{b0}$  obtained by Eq. (8). The predicted values of  $D_{b0}$  agreed well with the extrapolated  $D_b$  to  $h=0$ .

On the other hand, Mori and Wen<sup>14)</sup> derived the maximum bubble diameter from the mass balance of gas by assuming that no coalescence can occur sufficiently high above the distributor when the distance between the leading and the following bubbles is larger than  $4D_b$ . Their results are formulated by

$$D_{bm} = 1.64 \{ (u_0 - u_{mf}) A_t \}^{0.4} \quad (9)$$

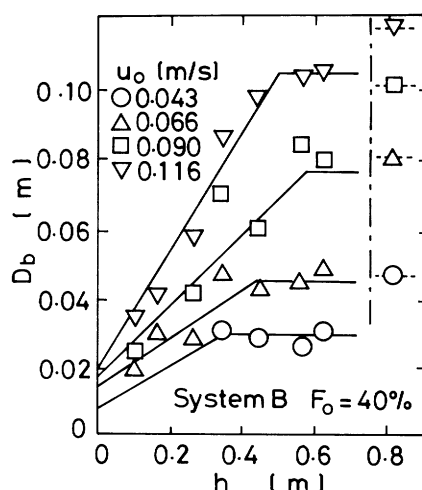


Fig. 6. Typical plot of  $D_b$  against  $h$

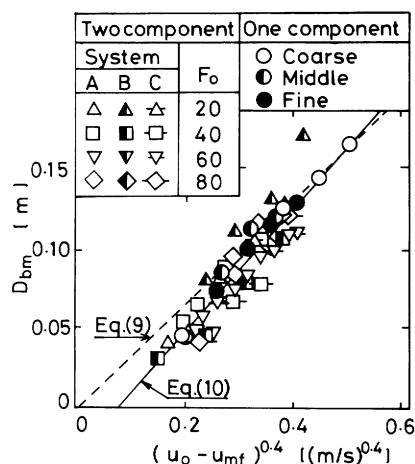


Fig. 7.  $D_{bm}$  and its correlation by Mori *et al.*

The keys with dotted lines on the right-hand side in Fig. 6 show the maximum attainable bubble diameter as calculated by Eq. (9). In contrast with the good agreement between predicted and experimental values of  $D_{b0}$ ,  $D_{bm}$ 's are overestimated by Eq. (9). In the fluidized beds formed by group A particles of Geldart<sup>5)</sup>, it is reported that the maximum attainable bubble diameters became smaller than the  $D_{bm}$ 's predicted by Eq. (9), because the splitting of the bubble is not negligible<sup>8)</sup>. However, it is not satisfactory to say that the difference between observed and calculated maximum attainable bubble diameters is owing solely to the splitting, because only fine particle in our experiments barely belongs to Geldart's group A. This suggests that the bubble diameter with a combination of two kinds of component particles is equal to that with a single kind of component particle at the time of bubble generation, while the rates of bubble growth are not the same.

Therefore, for the two-component system we try to obtain a new correlation between  $(u_0 - u_{mf})$  and  $D_{bm}$ . Figure 7 shows the  $D_{bm}$  change against  $(u_0 - u_{mf})^{0.4}$ ,

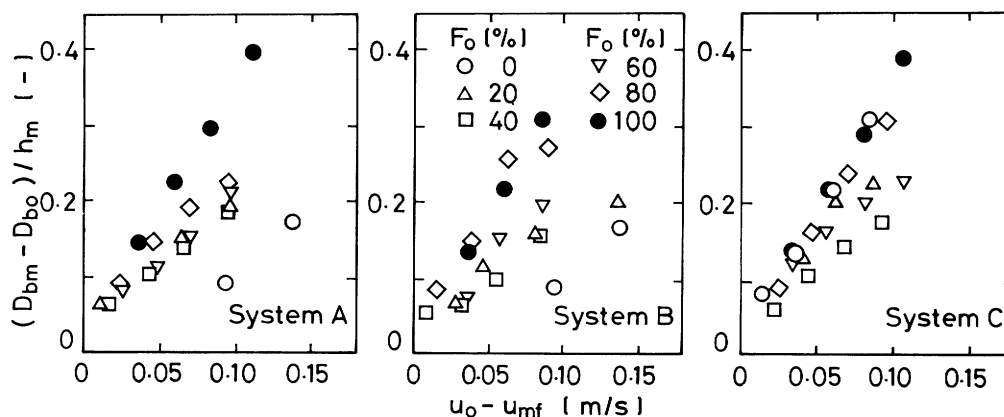


Fig. 8. Bubble growth ratio in one- or two-component particles

where the dotted line is drawn according to Eq. (9) in order to compare the two component particles. It is interesting to note that Eq. (9) can fit the results for the single-component system better than those for the two-component system.

From Fig. 7 we propose the following equation to estimate  $D_{bm}$ ; it covers all experimental conditions introduced in this report for the two-component system.

$$D_{bm} = -0.028 + 0.373(u_0 - u_{mf})^{0.4} \quad (10)$$

#### 4.4 Bubble growth ratio

Noting the linearity of bubble growth as seen at  $h$  smaller than  $h_m$  in Fig. 6,  $(D_{bm} - D_{b0})/h_m$  was regarded as a bubble growth ratio and is shown against  $(u_0 - u_{mf})$  in Fig. 8. It is interesting to note that the bubble growth ratios in the one-component system ( $F_0 = 0$  and 100) are different from those in the two-component system where  $F_0$  of about 40% takes a minimum bubble growth ratio. This smallest bubble growth ratio may relate to the fact that the voidage of the fixed bed takes a minimum at about 40% finer particles in the two-component system<sup>10)</sup> and that the apparent viscosity of a fluidized bed of binary spherical particle mixture has a maximum point at an abnormal composition<sup>6)</sup>.

Though no clear rule has been found between  $F_0$  and the bubble growth ratio, the feature of Fig. 8 is very similar to that of Fig. 5. This similarity suggests that the bubble growth ratio is very closely related to  $u_b$ . The bubble rising velocity strongly depends on the mobility of the particles in the bed, so  $u_b$  is considered to be affected by the fluidity of the bed particles. Then we regard  $u_b$  as one index which represents the fluidity in the fluidized bed.

Since it is difficult to know the acceleration rate of the following bubble when coalescence, and splitting in some cases, occurs, we have tried to correlate  $\bar{u}_b$ , the average value of rising velocities of bubbles below the height  $h_m$ , to  $(D_{bm} - D_{b0})/h_m$ .  $(D_{bm} - D_{b0})/h_m$  is

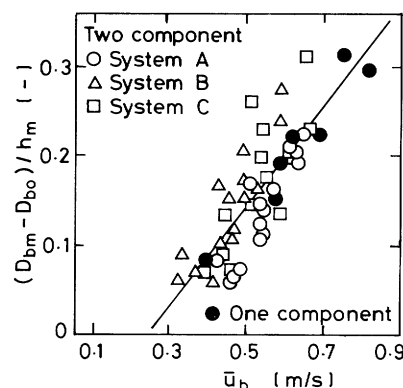


Fig. 9. Correlation between  $(D_{bm} - D_{b0})/h_m$  and  $\bar{u}_b$

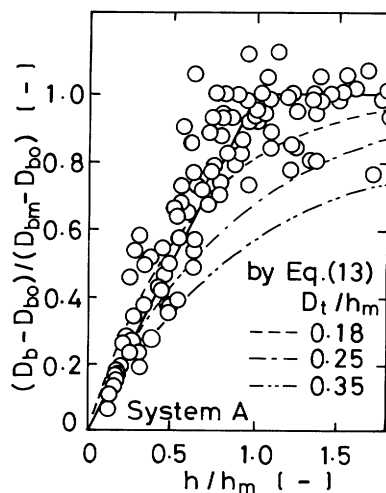


Fig. 10.  $(D_b - D_{b0})/(D_{bm} - D_{b0})$  vs.  $h/h_m$

plotted against  $\bar{u}_b$  in Fig. 9, from which it is found that the bubble growth ratio is proportional to the average bubble rising velocity and is approximately expressed in dimensional terms as follows.

$$(D_{bm} - D_{b0})/h_m = -0.128 + 0.525\bar{u}_b \quad (11)$$

In Fig. 10,  $(D_b - D_{b0})/(D_{bm} - D_{b0})$  is plotted against  $h/h_m$ .  $(D_b - D_{b0})/(D_{bm} - D_{b0})$  represents the axial

growth rate of  $D_b$  from  $D_{b0}$  to  $D_{bm}$ . It is seen that

$$(D_b - D_{b0}) / (D_{bm} - D_{b0}) = h / h_m \quad \text{when } 0 < h/h_m < 1 \quad (12-1)$$

and

$$(D_b - D_{b0}) / (D_{bm} - D_{b0}) = 1 \quad \text{when } h/h_m \geq 1 \quad (12-2)$$

in spite of the variations of  $u_0$  and  $F_0$ . Also, no difference among the systems can be observed. Mori and Wen<sup>14)</sup> have proposed the following equation for estimating  $D_b$  at  $h$ .

$$\frac{D_b - D_{b0}}{D_{bm} - D_{b0}} = 1 - \exp\left(-0.3 \frac{h/h_m}{D_t/h_m}\right) \quad (13)$$

The broken lines in Fig. 10 are drawn according to Eq. (13), taking  $h_m/D_t$  as the parameter. From Fig. 10, it is found that Eq. (13) cannot describe the bubble growth in a two-component fluidized bed system.

Many investigators<sup>8,9,11,12,19,20)</sup> have proposed models and examined them to clarify the mechanism of coalescence and splitting of bubbles. But the mechanism is too complex to understand because of the complexity of fluidity in the bed and many other factors that must be taken into consideration. Further, there have been few papers in which the effect of  $F_0$  on the bubble behavior of a multi-solid fluidized bed system is systematically investigated. For all two-component systems examined, however, it is found that even if the values of  $D_{b0}$ ,  $D_{bm}$  and  $h_m$  are not the same for each system and each  $F_0$ , the pattern of bubble growth is analogous, as shown in Fig. 10.

#### 4.5 A method for estimating bubble diameters in the two-component system

Now we can estimate the bubble diameter at any height in a two-component fluidized bed by use of the result mentioned above. The procedure is as follows:

1. Determine operating conditions,  $u_0$ ,  $A_t$  and  $n_{or}$ .
2. Measure the minimum fluidization velocity  $u_{mf}$  and observe  $u_b$  at a few and/or several points below  $h_m$  by any method to obtain their mean value  $\bar{u}_b$ .
3. Calculate  $D_{b0}$  and  $D_{bm}$  by Eqs. (8) and (10), respectively.
4. Determine  $h_m$  with  $D_{bm}$ ,  $D_{b0}$  and  $\bar{u}_b$  by means of Eq. (11).
5. Obtain  $D_b$  at any height  $h$  by Eq. (12).

Figure 11 shows the relationship between the calculated  $D_b$  by this procedure and the experimental data. The experimental data were estimated by the proposed method within  $\pm 20\%$  accuracy.

#### Conclusion

Observations of bubble behavior in systems of two kinds of component particles were conducted by

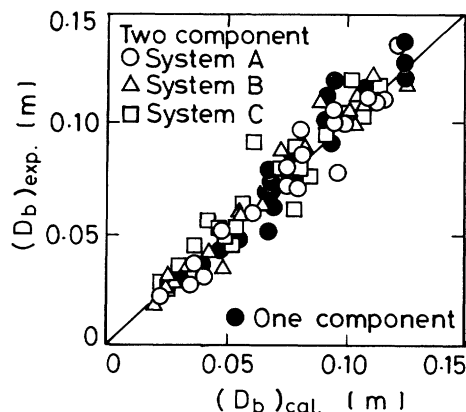


Fig. 11. Comparison between calculated and experimental values of  $D_b$ .

changing the weight percentages of finer particles. The following conclusions were reached.

- (1) Bubble diameters increase linearly up to a maximum attainable diameter.
- (2) Although  $D_{bm}$  by Mori and Wen's<sup>14)</sup> theory interprets the results well for systems of single-component particles, it deviates a little in the case of two-component systems.
- (3) The bubble growth ratio  $(D_{bm} - D_{b0})/h_m$  is at a minimum at  $F_0$  of about 40% and can be correlated better by the bubble rising velocity than by  $F_0$ . This bubble rising velocity is regarded as an index representing the fluidity of bed particles.
- (4) A method for determining the bubble diameter for systems of two kinds of component particles is proposed.

#### Nomenclature

$A_t$	= cross-sectional area of distributor	[m <sup>2</sup> ]
$a, b, c$	= constants in Eq. (4)	[m, m <sup>1-c</sup> , —]
$D_b$	= bubble diameter defined by Eq. (6)	[m]
$D_{b0}$	= incipient bubble diameter	[m]
$D_{bm}$	= maximum attainable bubble diameter	[m]
$D_t$	= diameter of bed	[m]
$d_p$	= diameter of particle	[μm]
$E$	= relative error between $u_{mf}$ and $u'_{mf}$	[%]
$F_0$	= weight percentage of finer particles	[%]
$h$	= height above distributor	[m]
$h_m$	= height above distributor where bubble attains maximum	[m]
$n_{or}$	= number of nozzles in distributor	[—]
$r$	= radius	[m]
$t$	= thickness of two-dimensional bed	[cm]
$u_b$	= bubble rising velocity	[m/s]
$\bar{u}_b$	= average bubble rising velocity below $h_m$	[m/s]
$u_c$	= minimum fluidization velocity of bed of coarser particles	[m/s]
$u_f$	= minimum fluidization velocity of bed of finer particles	[m/s]
$u_{mf}$	= minimum fluidization velocity	[m/s]
$u'_{mf}$	= minimum fluidization velocity by Eq. (7)	[m/s]
$u_0$	= superficial gas velocity	[m/s]
$V_b$	= volume of bubble	[m <sup>3</sup> ]
$x$	= coordinate in Fig. 2	[m]

$z$	= vertical bubble void	[m]
$z_2$	= maximum bubble height measured on picture of two-dimensional bed	[m]
$z_{2p}$	= bubble height defined by Eq. (1)	[m]
$z_3$	= maximum bubble height measured on picture of three-dimensional bed	[m]
$z_{3p}$	= bubble height defined by Eq. (3)	[m]
$\Delta$	= difference	
$\theta$	= angle in Fig. 3	[—]
—	= average	

#### Literature Cited

- Cheung, L., Nienow, A. W. and P. N. Rowe: *Chem. Eng. Sci.*, **29**, 1301 (1974).
- Chiba, T., K. Terashima and H. Kobayashi: *J. Chem. Eng. Japan*, **6**, 78 (1973).
- Darton, R. C., R. D. LaNauze, J. F. Davidson and D. Harrison: *Trans. Instn Chem. Engrs*, **55**, 274 (1977).
- Geldart, D.: *Powder Tech.*, **4**, 41 (1970/1971).
- Geldart, D.: *Powder Tech.*, **7**, 285 (1973).
- Hagyard, T. and A. M. Sacerdote: *I.E.C. Fund.*, **5**, 500 (1966).
- Hirama, T., M. Ishida and T. Shirai: *Kagaku Kogaku Ronbunshu*, **1**, 272 (1975).
- Horio, M. and A. Nonaka: *AIChE J.*, **33**, 1865 (1987).
- Kato, K. and C. Y. Wen: *Chem. Eng. Sci.*, **24**, 1351 (1969).
- Kunii, D. and O. Levenspiel: "Fluidization Engineering," p. 71, John Wiley & Sons, N.Y. (1969).
- Leung, L. S.: *Powder Tech.*, **6**, 189 (1972).
- Lin, S. P.: *AIChE J.*, **16**, 130 (1970).
- Miwa, K., S. Mori, T. Kato and I. Muchi: *Kagaku Kogaku*, **35**, 770 (1971).
- Mori, S. and C. Y. Wen: *AIChE J.*, **21**, 109 (1975).
- Rowe, P. N. and B. A. Partridge: *Trans. Instn Chem. Engrs*, **43**, T157 (1965).
- Rowe, P. N.: *Chem. Eng. Sci.*, **31**, 285 (1976).
- Rowe, P. N. and H. Masson: *Trans. Instn Chem. Engrs.*, **59**, 177 (1981).
- Toei, R., R. Matsuno, H. Kojima, Y. Nagai, K. Nakagawa and S. Yu: *Kagaku Kogaku*, **29**, 851 (1965).
- Toei, R., R. Matsuno, M. Oichi and K. Yamamoto: *J. Chem. Eng. Japan*, **7**, 451 (1974).
- Toei, R. and R. Matsuno: Int. Symp. on Fluidization, Eindhoven, Netherlands, 4-2-1 (1976).